

Figure 3. Stimulated echo (also known as Mims) pulsed ENDOR spectrum of C_{60} in fuming sulfuric acid. Experimental conditions: microwave frequency, 9.0250 GHz; magnetic field, 3231.0 G; microwave pulse widths, 0.05 μ s; delay between pulses one and two, 0.30 μ s; rf pulse width, 12.0 μ s; pulse sequence repetition rate, 167 Hz; rf step increment, 0.1 MHz; sweep size, 301 points.

^1H peak from the solvent protons is observed. There is no evidence for larger ^1H or ^{13}C couplings. This rules out the possibility that the shoulders in the ESR spectrum could arise from ^1H or ^{13}C hyperfine interactions.¹⁴ The small peak at the ^{19}F Larmor frequency in Figure 3 arises from the dipolar coupling to SO_2FCl .

The triplet signal intensity reaches a maximum after roughly 2 h while the total integrated ESR susceptibility increases by roughly a factor of 5 after approximately 4 h at room temperature following the initial mixing at 263 K. As a rough estimate, and assuming $S = 1/2$, a maximum of 0.5 spins/ C_{60} is observed. Since the characteristic UV/visible absorptions associated with neutral C_{60} ¹⁵ are not observed at any time, including immediately after the initial mixing at 263 K, the calculated spin density indicates that a significant portion of oxidized C_{60} exists as an ESR-silent (and likely diamagnetic) species. This is consistent with our earlier findings for C_{60} in Magic Acid.⁶

Explanations for the observed triplet-state ESR signal must account for the following experimental observations: a g -value of 2.003; a small (axial) $|D|$ value which is temperature independent between 4 and 110 K; the small ^{13}C hyperfine coupling; and a short electron spin lattice relaxation time, T_{1e} , compared to that observed for the monoradical of C_{60} . Furthermore, assuming that $|D|$ arises from the spin-spin interactions and localized electrons, a first-order approximation for the average distance (r) separating the two electrons,¹⁶ $\langle r \rangle^3 (\text{\AA}) = 6954g^2/|D(G)|$, yields $\langle r \rangle = 9.65 \text{ \AA}$. This is close to the van der Waals radius for the C_{60} molecule¹⁷ and is consistent with two spins on opposite sides of the soccerball cage.¹⁸ The 5-fold-degenerate HOMO of the neutral C_{60} molecule would be expected to undergo a Jahn-Teller distortion after oxidation to the C_{60}^{n+} ion with $n \geq 2$ in a triplet spin state. A Jahn-Teller distortion is consistent with the shorter T_{1e} value observed for the triplet signal. A distortion to an elliptically elongated soccerball structure would also be consistent with the slightly larger (r) value.

(14) The weakly coupled ^{13}C nuclei observed in the ESEEM spectrum are not observed in the pulsed ENDOR spectrum because pulse conditions were used to optimize the observation of ^{13}C and ^1H nuclei with larger hyperfine couplings. For details, see: Thomann, H.; Bernardo, M. *Spectroscopy (Ota-awa)* **1990**, *8*, 119.

(15) Intense band at 330 nm, weak band at 406 nm.

(16) Abragam, A.; Bleaney, B. *Electron Paramagnetic Resonance of Transition Metal Ions*; Clarendon Press: Oxford, 1970; p 492.

(17) (a) Hawkins, J. M.; Meyer, A.; Lewis, T. A.; Loren, S.; Hollander, F. J. *Science* **1991**, *252*, 312. (b) Fagan, P. J.; Calabrese, J. C.; Malone, B. *Science* **1991**, *252*, 1160.

(18) The distance between diametrically opposed carbon atoms is ca. 7 \AA . The distance between the carbon π electron cloud on diametrically opposed carbons is roughly 8.5 \AA . This latter distance is the more pertinent number for comparison to the (r) value derived from the zero field splitting, $|D|$.

Considering that C_{60} is irreversibly oxidized by electrochemical means with a loss of four electrons,¹⁹ it is tempting to suggest the formation of a Jahn-Teller distorted diradical tetracation with a filled doubly degenerate state below a partially filled triply degenerate HOMO. It is possible, however, that lower oxidation states of C_{60} (e.g., the diradical dication of C_{60} , $C_{60}^{2+,2+}$) are stabilized in the superacid solution and are giving rise to the observed triplet. In either case, the temperature dependence of the EPR signal suggests that the triplet state is the ground state of the C_{60}^{n+} diradical dication. Work continues in our laboratory to sort through these possibilities.

(19) Dubois, D.; Kadish, K. M.; Flanagan, S.; Wilson, L. J. *J. Am. Chem. Soc.* **1991**, *113*, 7773.

Partial Structures of Maitotoxin, the Most Potent Marine Toxin from Dinoflagellate *Gambierdiscus toxicus*

Michio Murata,[†] Takashi Iwashita,[‡] Akihiro Yokoyama,[†] Masahiro Sasaki,[†] and Takeshi Yasumoto*[†]

Faculty of Agriculture, Tohoku University
Tsutsumidori-Amamiyamachi, Aoba-ku
Sendai 981, Japan

Suntory Institute for Bioorganic Research
Shimamoto-cho, Mishima-gum, Osaka 618, Japan

Received April 6, 1992

Maitotoxin (MTX) has been found to be one of the causative toxins of ciguatera, a poisoning caused by ingestion of coral reef fish.¹ In lethal potency (mouse, ip.) MTX exceeds tetrodotoxin by a factor of 200, making it the most potent nonproteinaceous toxin known. The toxin has attracted the attention of biochemists and pharmacologists due to its powerful ability to stimulate Ca^{2+} influx across biomembranes.² Recently, other biological activities were discovered,³ such as phosphoinositide breakdown⁴ and activation of protein kinases,⁵ some of which are not directly linked to elevation of Ca^{2+} levels. As a natural product, MTX is also well-known for its complex structure and molecular weight (3424 Da),⁶ which exceeds that of palytoxin by 748 Da. Thus MTX is one of the most challenging structural targets in natural product chemistry.

Despite our efforts to elucidate the structure of MTX for over 15 years, we have succeeded only in establishing small structural moieties.⁶ In this communication, we wish to report a partial structure of MTX (**1**) which accounts for 30% of the weight of the molecule.

MTX was extracted from cultured cells of *Gambierdiscus toxicus* and purified as reported previously.⁶ Approximately 25 mg (7.3 μ mol) of MTX was obtained from 5000 L of culture. Extensive measurements of two-dimensional NMR spectra⁷ were carried out, including ^1H - ^1H COSY, 2D HOHAHA, DQF-COSY, NOESY, ^1H - ^{13}C COSY, HMQC, HMBC, and the recent techniques of HSQC and 2D HMQC/HOHAHA. However, overlapping as well as poor resolution of both ^{13}C and ^1H NMR signals due to the large molecular size prevented us from applying routine methods for structural analyses. In particular, the NMR

[†]Tohoku University.

[‡]Suntory Institute for Bioorganic Research.

(1) Yasumoto, T.; Bagnis, R.; Vernoux, J. P. *Bull. Jpn. Soc. Sci. Fish.* **1976**, *42*, 359-365.

(2) Takahashi, M.; Ohizumi, Y.; Yasumoto, T. *J. Biol. Chem.* **1982**, *257*, 7287-7289.

(3) Gusovsky, F.; Daly, J. W. *Biochem. Pharmacol.* **1990**, *39*, 1633-1639.

(4) Berta, P.; Sladeczek, F.; Derancourt, J.; Durand, M.; Travo, P.; Haiech, J. *FEBS Lett.* **1986**, *197*, 349-352.

(5) Gusovsky, F.; Daly, J. W. Personal communication.

(6) Yokoyama, A.; Murata, M.; Oshima, Y.; Iwashita, T.; Yasumoto, T. *J. Biochem.* **1988**, *104*, 184-187.

(7) All 2D NMR spectra were recorded either on a GN-500 (500 MHz, General Electric) or a GSX-400 (400 MHz, JEOL) spectrometer except for 2D HMQC-HOHAHA, which was measured on an Omega-500 (500 MHz, General Electric) instrument.

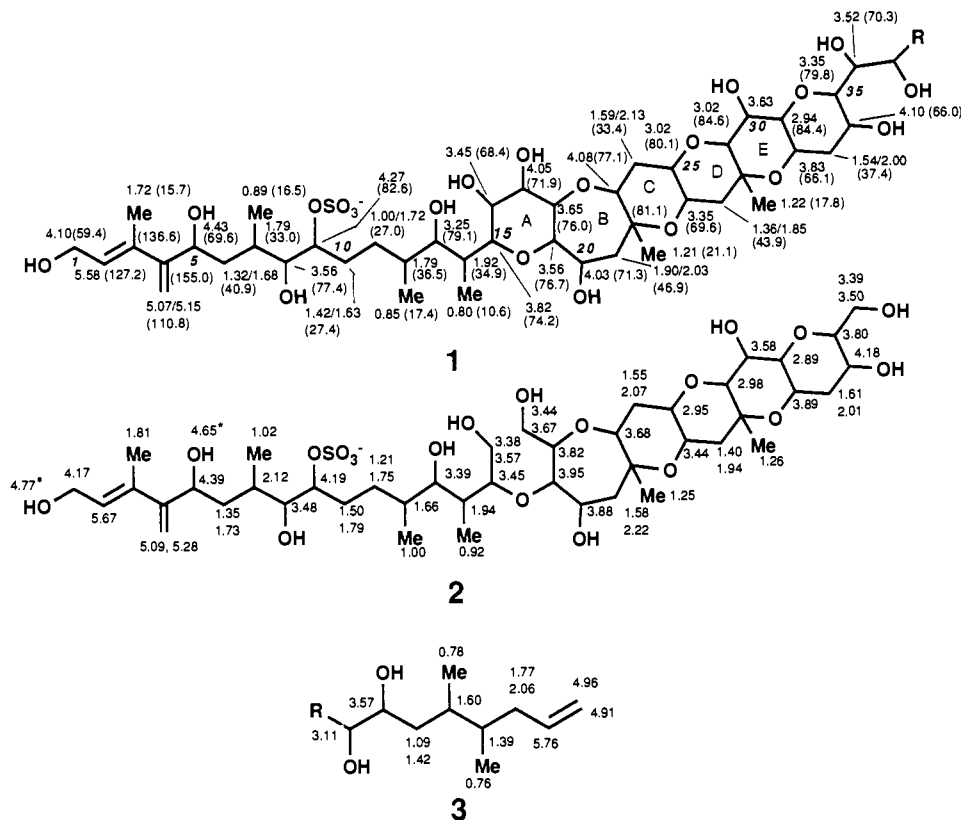


Figure 1. Structures and NMR assignments of terminal segments of MTX (**1** and **3**) and a periodate degradation product (**2**). ^1H NMR chemical shifts of **1** and **3** and ^{13}C NMR (in parentheses) shifts of **1** are those in $\text{CD}_3\text{CN}-\text{D}_2\text{O}$ (2:1). ^1H NMR spectra of **2** were measured in $(\text{CD}_3)_2\text{SO}$ at 50°C except for those with asterisks (at 23°C).

signals arising from the central part of the molecule tended to be broadened because of the predominance of fused cyclic ethers. Thus, correlations due to $^3J_{\text{H,H}}$ or $^2J_{\text{C,H}}$ were weak or absent from the $^1\text{H}-^1\text{H}$ COSY or HMBC spectra. Fortunately, the absence of repeating units or symmetrical moieties near the C1 terminus made the 2D spectra more informative and resulted in successful elucidation of partial structure **1** (C1–C37).

The presence of two sulfate esters in MTX was previously deduced by FABMS of the desulfated product (ds-MTX).⁶ The position of one sulfate was assigned to C9 by comparison of COSY spectra of ds-MTX with MTX. The location of hydroxyl groups was determined mainly by combined use of $^1\text{H}-^{13}\text{C}$ COSY spectra and deuterium shifts in ^{13}C NMR signals.⁸ The six ether rings in the partial structure were assigned on the basis of NOEs observed as intense cross-peaks in NOESY spectra between H15/H19, H18/H23, Me-C22/H26, H25/H29, Me-C28/H32, and H31/H35. NOESY experiments provided essential information not only for connectivities around the ether bonds but also for correlating structural data vicinal to quaternary carbons (C22 or C28).

Partial structure **1** was confirmed by its periodate degradation products.⁹ HPLC and structural data obtained by NMR suggested that the molecule was cleaved into three parts. The first fragment, A (**2**), showed an $(\text{M} - \text{Na})^-$ peak at m/z 941 by FABMS. The structure of **2** was solved with $100\ \mu\text{g}$ of the sample. $^1\text{H}-^1\text{H}$ COSY spectra successfully led to the assignment of all ^1H NMR resonances (Figure 1). The chemical shifts agreed well

with those of intact MTX except for protons near the cleavage sites. The relatively large difference in ring B resonances is explained by conformational changes in the ring and by a change in the orientation of C17 and C20 hydroxyl groups resulting from bond cleavage at C16/C17.

Fragment C (**3**), the other terminal segment, is small with a molecular weight of 142. Its structure was readily deduced from NMR data (Figure 1), although a degradation product could not be obtained because of its extremely small amount and high volatility.

Fragment B is derived from the middle part of MTX and has the largest molecular weight. By subtracting the molecular weights of **1** and **3** from the weight of MTX, the approximate molecular weight of fragment B was estimated to be 2300 Da. ^1H NMR spectra of fragment B showed 13 angular methyls on ether rings, implying that the fragment consisted principally of fused cyclic ethers as found in the brevetoxins.¹⁰ The number of rings in this fragment was estimated to be 22–27 on the basis of $^1\text{H}-^{13}\text{C}$ COSY spectra and deuterium shifts observed in ^{13}C NMR signals.¹¹ Hence, MTX contains 28–33 ether rings.

The present study has demonstrated that MTX has a polyether skeleton similar to brevetoxin, encompassing approximately 30 ether rings, 30 hydroxyls, 21 methyls, and 2 sulfate esters. The half of the molecule which includes fragment A is relatively hydrophilic, while the other half, comprising mostly contiguous fused rings, is hydrophobic, thus accounting for the dual polarity of the toxin.

Acknowledgment. We are grateful to Dr. M. Oyabu of Shimadzu Corporation for NMR measurements, including 3D and

(8) The ^{13}C NMR spectra (broad band ^1H decoupling) were measured in $\text{CD}_3\text{CN}-\text{H}_2\text{O}$ and in $\text{CD}_3\text{CN}-\text{D}_2\text{O}$. Hydroxyl-bearing carbons were shifted by -0.08 to -0.1 ppm due to deuterium exchange. Positions of hydroxyls were partly confirmed by observing $^3J_{\text{H,H}}$ in **2** as shown in Figure 1.

(9) Periodate degradation was carried out with $1.5\ \text{mg}$ of MTX ($0.44\ \mu\text{mol}$) in $50\ \mu\text{L}$ of $40\ \text{mM}$ NaIO_4 , followed by NaBH_4 reduction (large excess) in MeOH. HPLC on a reversed-phase column (Rosil TMS, BioRad) using gradient elution with MeCN in $5\ \text{mM}$ potassium phosphate buffer yielded ca. $100\ \mu\text{g}$ of **2** and ca. $200\ \mu\text{g}$ of fragment B, together with complex mixtures of structurally similar fragments.

(10) (a) Lin, Y.-Y.; Risk, M.; Ray, S. M.; Engon, D. V.; Clardy, J.; Golik, J.; James, J. C.; Nakanishi, K. *J. Am. Chem. Soc.* **1981**, *103*, 6773–6775. (b) Shimizu, Y.; Chou, H.-N.; Bando, H.; Duyn, G. V.; Clardy, J. *J. Am. Chem. Soc.* **1986**, *108*, 514–515.

(11) $^1\text{H}-^{13}\text{C}$ COSY and deuterium shift experiments⁸ revealed that, of approximately 70 carbons bearing oxygen in fragment B, approximately 50 are ether carbons and 20 bear hydroxyl groups.

2D HMQC/HOHAHA, and to Dr. Wälchli of Japan Bruker for NMR measurements. We thank Drs. H. Naoki of Suntory Institute, K. Tanaka of JEOL Co. for measuring mass spectra, and Prof. P. J. Scheuer, University of Hawaii, for discussions. The work was supported in part by a grant-in-aid from the Ministry of Education, Science, and Culture, Japan, and by the Naito Foundation.

Supplementary Material Available: ^1H - ^1H COSY, ^1H - ^1H HOHAHA, NOESY, and ^1H - ^{13}C HOHAHA spectra of MTX and ^1H - ^1H COSY spectrum of fragment A (5 pages). FABMS and ^{13}C NMR spectra have been published previously.⁶ Ordering information is given on any current masthead page.

Palladium-Catalyzed Ring-Opening Copolymerization of Cyclopolysilanes and Cyclic Disilanes with *p*-Quinones

N. Prabhakar Reddy, Hiroshi Yamashita, and Masato Tanaka*

National Chemical Laboratory for Industry
Tsukuba, Ibaraki 305, Japan

Received April 23, 1992

Organosilicon polymers such as polysiloxanes, polycarbosilanes, polysilazanes, and polysilanes have attracted increasing attention for their current and future engineering applications.¹ In this sense, new and efficient methods for their preparation have been highly desired. However, ring-opening polymerization is still very rare except for the reaction of cyclic siloxanes, and only a few examples of strained cyclic disilanes² and cyclotetrasilanes³ have been reported for Si-Si bond-containing polycarbosilanes and polysilanes. We report herein an entirely new and rather unusual copolymerization of cyclopolysilanes and cyclic disilanes with *p*-quinones to afford regular polymers consisting of *p*-(arylene-dioxy)silylene linkages.

A mixture of dodecamethylcyclohexasilane (**1a**, 0.10 mmol), 1,4-naphthoquinone (**2a**, 0.66 mmol), $\text{PdCl}_2(\text{PET}_3)_2$ (0.008 mmol), and benzene (0.10 mL) was heated at 120 °C for 14 h in a sealed tube under nitrogen. ^1H NMR spectroscopy showed clean conversion of the Me signal at 0.07 ppm arising from **1a** into a new rather broad signal at 0.08–0.66 ppm. The resulting mixture was dissolved in benzene (5 mL) and filtered. Concentration of the filtrate to about 1/5 followed by addition of 2-propanol gave a pale gray solid of poly[1,4-naphthylenedioxy]dimethylsilylene (**3a**)^{4a} (eq 1) in 60% yield. The molecular weight (M_w) of **3a** was

(1) (a) *Inorganic and Organometallic Polymers*; Zeldin, M., Wynne, K. J., Allcock, H. R., Eds.; ACS Symposium Series 360; American Chemical Society: Washington, DC, 1988. (b) *Silicon Chemistry*; Corey, E. R., Corey, J. Y., Gaspar, P. P., Eds.; Ellis Horwood: Chichester, England, 1988. (c) *Silicon-Based Polymer Science*; Zeigler, J. M., Fearon, F. W. G., Eds.; Advances in Chemistry Series 224; American Chemical Society: Washington, DC, 1990.

(2) (a) Shiina, K. *J. Organomet. Chem.* **1986**, *310*, C57. (b) Ishikawa, M.; Hasegawa, Y.; Hatano, T.; Kunai, A. *Organometallics* **1989**, *8*, 2741. (c) Ishikawa, M.; Hatano, T.; Horio, T.; Kunai, A. *J. Organomet. Chem.* **1991**, *412*, C31.

(3) (a) Gupta, Y.; Cypryk, M.; Matyjaszewski, K. *Polym. Prepr.* **1990**, *31*, 270. (b) Cypryk, M.; Gupta, Y.; Matyjaszewski, K. *J. Am. Chem. Soc.* **1991**, *113*, 1046. (c) Matyjaszewski, K.; Cypryk, M.; Frey, H.; Hrkach, J.; Kim, H. K.; Moeller, M.; Ruehl, K.; White, M. *J. Macromol. Sci. Chem.* **1991**, *A28*, 1151.

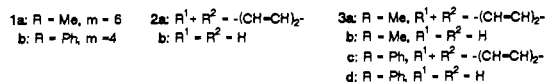
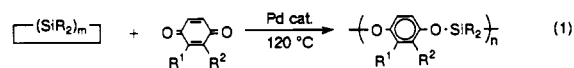
(4) Selected physical and spectral data of **3a**–**f** are as follows (mp, uncorrected; NMR CDCl_3 , δ). (a) **3a**: mp 88–92 °C; ^1H NMR 0.08–0.66 (br m, 6 H, SiCH_3) 6.76–7.19 (br m, 2 H, 2,3-ring H of $\text{OC}_{10}\text{H}_6\text{O}$), 7.41 (br s, 2 H, 5,8-ring H of $\text{OC}_{10}\text{H}_6\text{O}$), 8.09 (br s, 2 H, 6,7-ring H of $\text{OC}_{10}\text{H}_6\text{O}$). (b) **3b**: mp 115–120 °C; ^1H NMR 0.30 (s, 6 H, SiCH_3), 6.78 (s, 4 H, $\text{OC}_6\text{H}_4\text{O}$). (c) **3c**: mp 127–132 °C; ^1H NMR 6.60–6.85 (br m, 2 H, 2,3-ring H of $\text{OC}_{10}\text{H}_6\text{O}$), 6.92–7.52 (br m, 6 H, *m,p*-H of SiC_6H_5), 7.62–7.89 (br m, 4 H, *o*-H of SiC_6H_5), 7.92–8.38 (br m, 4 H, 5,6,7,8-ring H of $\text{OC}_{10}\text{H}_6\text{O}$). (d) **3d** (benzene-soluble fraction): mp 84–90 °C; ^1H NMR 6.50–6.83 (br m, 4 H, $\text{OC}_6\text{H}_4\text{O}$), 7.12–7.50 (br s, 6 H, *m,p*-H of SiC_6H_5), 7.53–7.82 (br m, 4 H, *o*-H of SiC_6H_5). **3d** (benzene-insoluble fraction): mp >300 °C. (e) **3e**: mp 43–46 °C; ^1H NMR 0.18 (s, 12 H, SiCH_3), 0.69 (t, $J = 7.6$, 4 H, SiCH_2), 1.29–1.49 (m, 4 H, SiCH_2CH_2), 6.66 (s, 4 H, $\text{OC}_6\text{H}_4\text{O}$). (f) **3f**: mp 110–120 °C; ^1H NMR 0.40 (br s, 12 H, SiCH_3), 6.11–6.33 (m, 4 H, $\text{OC}_6\text{H}_4\text{O}$), 6.48–6.71 (br m, 4 H of CC_6H_5), 6.85–7.19 (br m, 16 H of CC_6H_5).

Table I. Ring-Opening Copolymerization of 1,2-Disilacycles with *p*-Quinones^a

| 1,2-disilacycle | quinone | product | $M_w (M_w/M_n)^b$ | yield, % ^c |
|-----------------|-----------|-----------|--------------------------------------|-----------------------|
| 1a | 2a | 3a | 6.4×10^3 (2.1) | 60 |
| 1a | 2b | 3b | 2.1×10^4 (5.8) | 68 |
| 1b | 2a | 3c | 3.9×10^3 (2.2) | 76 |
| 1b | 2b | 3d | 1.7×10^4 (5.1) ^d | 41 |
| | | | 8.2×10^4 (11) ^e | 30 ^e |
| 1c' | 2b | 3e | 1.9×10^4 (3.9) | 65 |
| 1d' | 2b | 3f | 4.9×10^4 (3.6) | 71 |

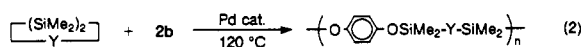
^a Reaction conditions: 1,2-disilacycle, 0.10 mmol; *p*-quinone, 1.10 equiv/Si-Si; $\text{PdCl}_2(\text{PET}_3)_2$, 0.008 mmol; benzene, 0.10 mL; 120 °C; 12–14 h. ^b Determined by GPC with polystyrene standards using THF as eluent at 40 °C. ^c Yield after purification by reprecipitation with benzene–2-propanol. ^d Bimodal peaks. ^e Benzene-insoluble fraction. ^f M_w and M_w/M_n were measured by high-temperature GPC using *o*-dichlorobenzene as eluent at 135 °C. ^g 0.4 mmol, 20 h. ^h Not purified.^{4f}

determined (by GPC with polystyrene standards) to be 6.4×10^3 ($M_w/M_n = 2.1$) (Table I). ^1H and ^{13}C NMR spectra^{4a} of **3a** are well conformed to the given structure, indicating a highly regular polymer consisting of alternating 1,4-naphthylenedioxy and dimethylsilylene units. Thus, the overall reaction involves ring opening of **1a**, insertion of **2a** into every Si-Si bond, and polymerization.



Similarly, **1a** reacted with *p*-benzoquinone (**2b**) to give poly-[(*p*-phenylenedioxy)dimethylsilylene] (**3b**).^{4b} Copolymerization of the somewhat congested octaphenylcyclotetrasilane (**1b**) with **2a** and **2b** also proceeded to give poly[(1,4-arylenedioxy)diphenylsilylene] polymers **3c**^{4c} and **3d**,^{4d,5,6} respectively. The polymers **3b** and **3d** obtained from **2b** have higher molecular weights than **3a** and **3c** obtained from **2a**. This may be because **2b** is sterically less demanding and thus more reactive than **2a**. Other catalyst systems such as $\text{PdCl}_2(\text{PPh}_3)_2$ and $\text{Pd}(\text{dba})_2 \cdot 2\text{P}(\text{OCH}_2)_3\text{Ct}$ (*dba* = dibenzylideneacetone) were also effective, although $\text{PdCl}_2(\text{PET}_3)_2$ seemed to be beneficial for obtaining polymers with high molecular weight; in the reaction of **1b** with **2b**, $\text{PdCl}_2(\text{PPh}_3)_2$ and $\text{Pd}(\text{dba})_2 \cdot 2\text{P}(\text{OCH}_2)_3\text{Ct}$ afforded only benzene-soluble polymers with M_w 's (M_w/M_n) of 2.0×10^4 (3.9) and 4.7×10^4 (5.1), respectively, while $\text{PdCl}_2(\text{PET}_3)_2$ gave a polymer that was partly insoluble in benzene (benzene-insoluble fraction; $M_w = 8.2 \times 10^4$, $M_w/M_n = 11$) (Table I).

The present reaction is applicable to cyclic disilanes as well. Thus, 1,1,2,2-tetramethyl-1,2-disilacyclohexane (**1c**) and 1,1,2,2-tetramethyl-3,4,5,6-tetraphenyl-1,2-disila-3,5-cyclohexadiene (**1d**) underwent 1/1 copolymerization with **2b** to give phenylenedioxy unit containing regular polymers **3e**^{4e} and **3f**,^{4f} respectively (eq 2, Table I).



A mechanism that involves neat ring-opening polymerization of the cyclic monomers and subsequent insertion of quinones into the Si-Si bonds in the backbone⁷ appears conceivable. However, the neat polymerization of **1a**–**c** did not take place ($\text{PdCl}_2(\text{PET}_3)_2$ catalyst, 120 °C, 14 h). On the other hand, the reaction of **1a** with phenanthraquinone gave a silylene adduct (**5**) in 46% yield

(5) The GPC curve of **3d** (benzene-soluble part) was bimodal: the area ratio of the higher fraction ($M_w = 3.2 \times 10^4$, $M_w/M_n = 1.8$) to the lower one ($M_w = 2.7 \times 10^3$, $M_w/M_n = 1.6$) was 0.8, suggesting the participation of at least two different copolymerization processes.

(6) Curry, J. E.; Byrd, J. D. *J. Appl. Polym. Sci.* **1965**, *9*, 295.

(7) We are finding rapid insertion of quinones into Si-Si bonds in polymer backbones. The results will be published elsewhere.